Supporting information for

On the Convective Self-Assembly of Colloidal Particles in Nanofluid Based on In-Situ Measurements of Interaction Forces

Nozomi Arai, Satoshi Watanabe*, and Minoru T. Miyahara**

Department of Chemical Engineering, Kyoto University, Katsura, Nishikyo, Kyoto 615-8510, Japan

*nabe@cheme.kyoto-u.ac.jp

**miyahara@cheme.kyoto-u.ac.jp

1. Detailed structure of nanoparticles

The interstitial space of the close-packed structure composed of microspheres is filled up with nanoparticles. The contact points between microspheres cannot be seen in SEM images shown in Fig. 4 in main text because they are buried under nanoparticles. To verify that microspheres form a close-packed structure, we fabricated particle films with a binary suspension of 6 μm silica particles and 85 nm polystyrene particles, and heated the resultant structure at 400 °C in 10 min to remove the polystyrene nanoparticles. Figure S1 shows SEM images of the structure before and after heating, which demonstrates that microspheres form a close-packed structure.

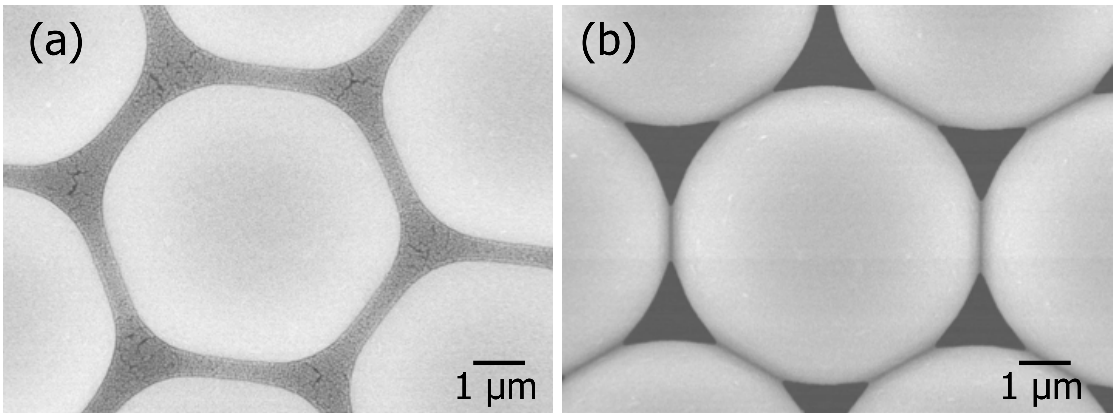

Figure S1. SEM images of the particle films fabricated with binary suspension of 6 μm silica particles and 85 nm polystyrene particles, (a) before heating and (b) after heating.

2. pH and ionic strength of suspensions used in fabricating particle films shown in Fig. 3

Table S1 shows the values of pH and ionic strength, I, of each nanofluid whose volume fraction is 0.02. In this series of experiments, pH and I were not adjusted. Hence nanofluids used for the film fabrication shown in Fig. 3 were in different conditions of pH and I because the original suspensions of nanoparticles (27, 45, and 90 nm) have different pH and I values.

Table S1. pH and ionic strength I of nanofluids.

Nanoparticle size	27 nm	45 nm	90 nm
pH	8.6	8.4	7.4
I [mM]	3.6	2.5	0.3

3. Particle film fabricated with 27 nm nanofluid of condition i) of pH = 6.3 and I = 1.2 mM

The particle film of microspheres fabricated with 27 nm nanofluid of condition i) (pH = 6.3, I = 1.2 mM) is shown in Fig. S2. Disordered multilayers due to aggregates of microspheres appear in particle films, which is in contrast to the particle film fabricated with 45 nm nanofluid of condition i) (Fig. 5b). In this case, the surface distance between microspheres is calculated to be 62 nm and shorter than that in 45 nm nanofluid of condition i) and 90 nm of condition ii) in which uniform structures without forming aggregates formed.

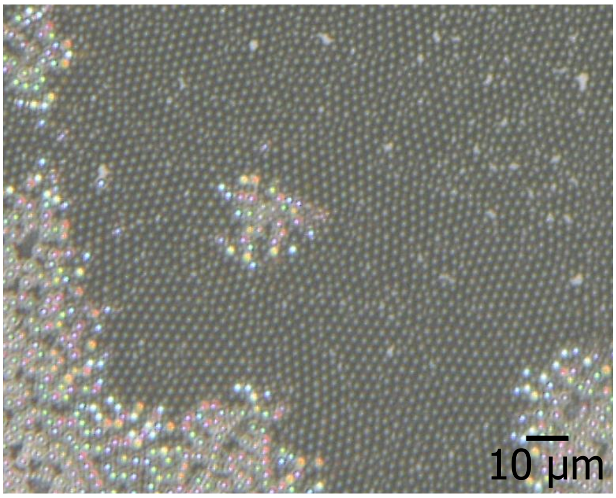

Figure S2. An optical microscope image of a particle film fabricated with 27 nm nanofluid of condition i) (pH = 6.3, I = 1.2 mM). V_w was 200 μm/s.

4. Force curves in pure water

We measured force curves in pure water to calculate the Debye length, and Figure S3 shows the result. The Debye length is 58 nm in pure water produced by a water purifier system in our laboratory (arium® mini, Sartorius AG, Germany). The ionic strength is 0.027 mM, which is determined by the following equation.

$$\frac{1}{\kappa} = \frac{0.3}{\sqrt{I}}$$

$1/\kappa$ is the Debye length, and I is the ionic strength. We also measured force curves in NaCl aqueous solutions to validate our measurements of force curves. The result in Fig. S3 demonstrates the decrease in the Debye length with I, the fact of which indicates the correctness of our interaction force measurements with AFM.

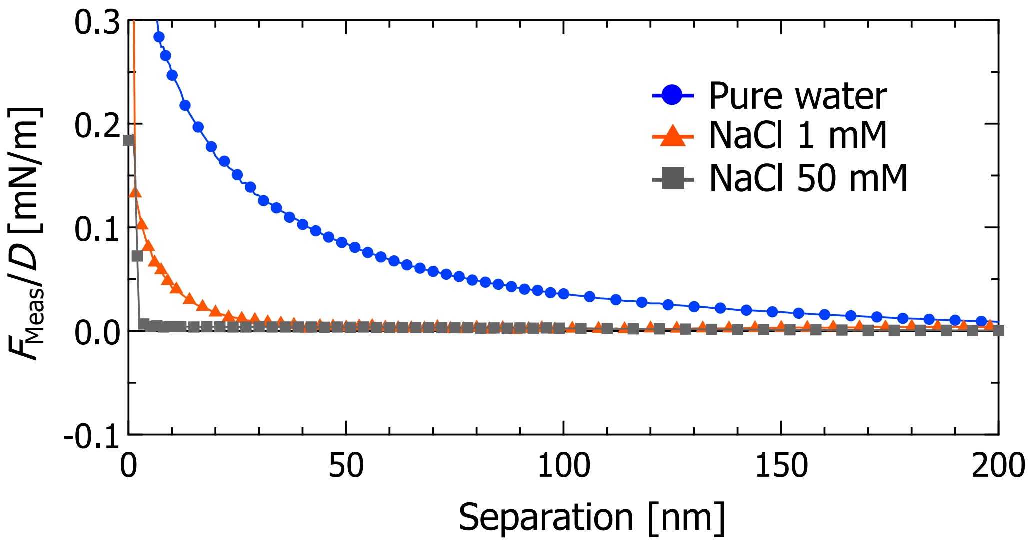

Figure S3. Force curves measured at 0.1 μm/s in pure water and aqueous solutions of NaCl.

5. The static force and verification of the hydrodynamic forces

Figure S4 shows the force curve measured with 0.5 μm/s shown in Fig. 6. There are the repulsive and attractive forces at short range. The attractive force shows a sharp change, which is asymmetric against the repulsive force. This feature of the attractive force at short range is characteristic the van der Waals force rather than the lubrication force. In contrast, force curves measured at higher velocities than 5 μm are dominated by the hydrodynamics because rescaling those force curves by the velocities V_{scan} collapse into a single master curve, and the master curve is fitted with a function in inverse proportion to the separation (black crosses) as shown in Fig. S5. It should be noted that there are deviations in short-ranged forces (less than 30 nm), possibly because the thin film of fluid is not completely ruptured in the case of higher velocities.

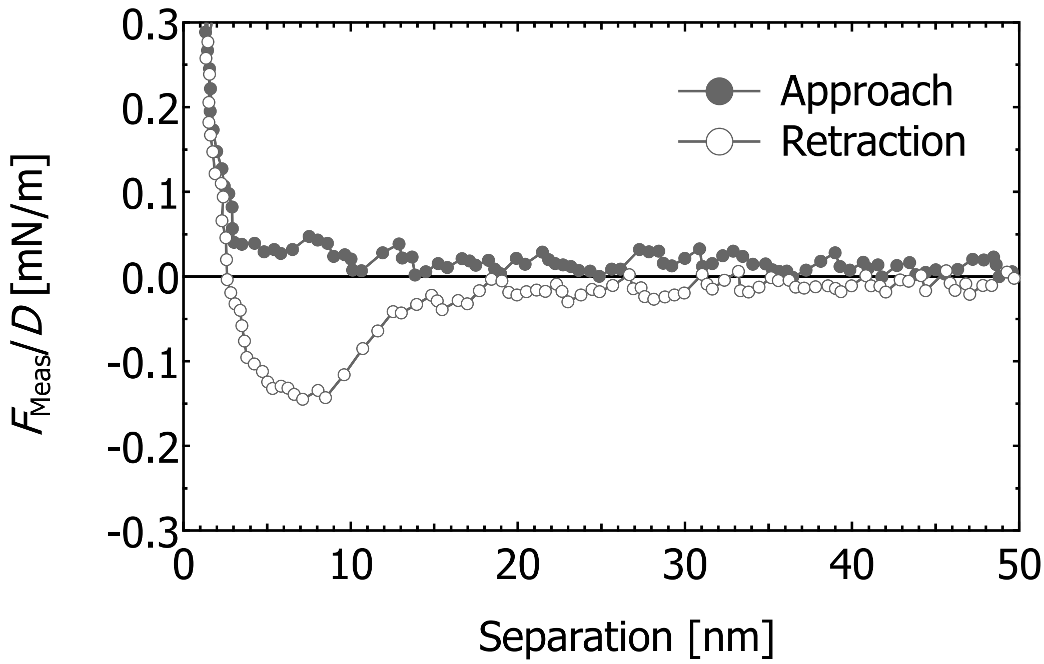

Figure S4. Force curves measured at 0.5 μm/s in a NaCl solution under the condition of pH = 10.1 and I = 70 mM.

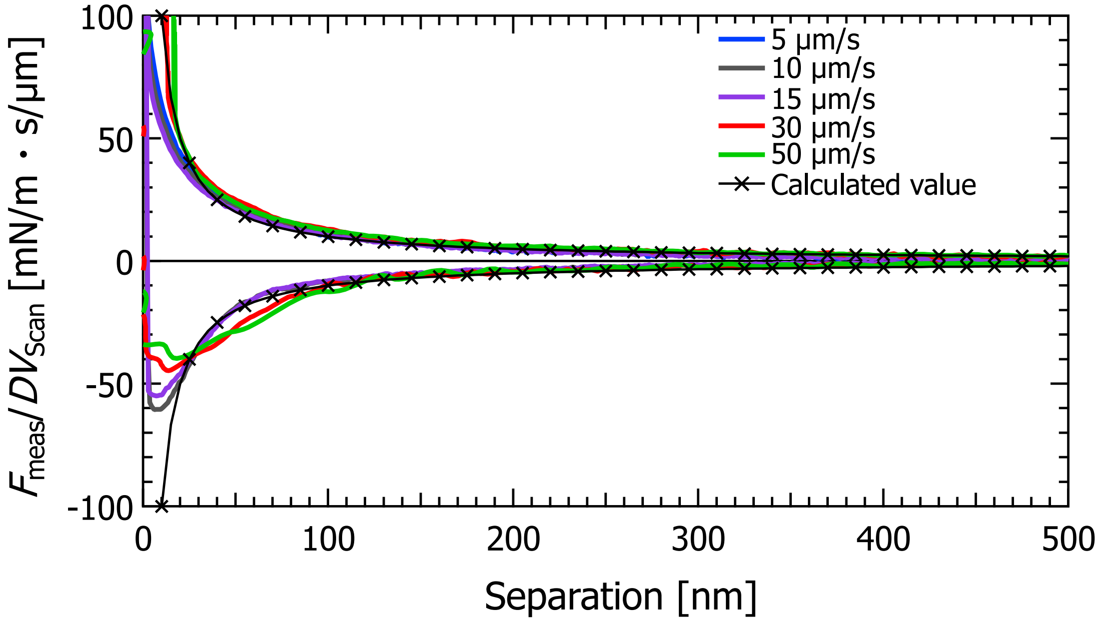

Figure S5. Force curves measured at 5-50 μm/s in a NaCl solution under the condition of pH = 10.1 and I = 70 mM.

6. The depletion force in nanofluids

Figure S6 shows the force curve measured in nanofluid of 27 nm nanoparticles under the condition of pH = 6.3 and I = 1.2 mM at a velocity of 0.5 μm/s. The oscillatory force that has been already reported in some previous works[1–4] was detected at short range in our measurements, and the attractive force has been reported as the depletion force in these studies. The magnitude of the depletion attraction was on the order of μN/m while the hydrodynamic force we focused in the main context is on the order of mN/m. Hence, we assume that the effect of the depletion force is less important in a high velocity region.

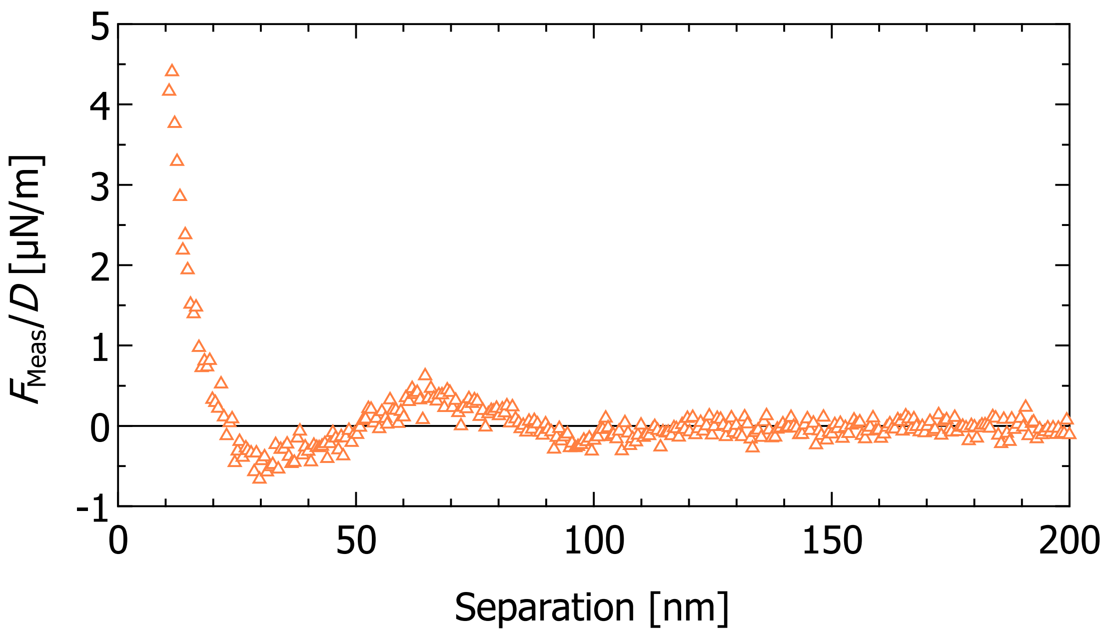

Figure S6. Force curves measured at 0.5 μm/s in nanofluid of 27 nm nanoparticles under the condition of pH = 6.3 and I = 1.2 mM.

7. Frequency distributions of the friction forces in nanofluids

Because nanoparticles scatter the laser beam used to detect the bending of the cantilever, negative friction forces in nanofluids can be recorded when scattered beams are detected. Additionally, when a colloidal probe climbs up or slips down the nanoparticles on a substrate, the cantilever can bend more than the contribution by friction forces. Hence, the frequency distributions in nanofluids are broadened. Because these errors must be isotropic, the median value of each distribution is not affected by these errors. It should be noted that each frequency distribution was calculated from 258 × 258 points of data. We assume that the number of the data points is sufficient in neglecting the statistical error.

8. Numerical data of force curves measured in an aqueous solution, nanofluids, and pure water

Table S2. Numerical data of force curves shown in Fig. 7.

Ions		27 nm nanofluid		45 nm nanofluid		90 nm nanofluid		Pure water	
x [nm]	$(F_{MEAS}\text{-}F_{Drag})$ / D [mN/m]	x [nm]	$(F_{MEAS}\text{-}F_{Drag})$ / D [mN/m]	x [nm]	$(F_{MEAS}\text{-}F_{Drag})$ / D [mN/m]	x [nm]	$(F_{MEAS}\text{-}F_{Drag})$ / D [mN/m]	x [nm]	$(F_{MEAS}\text{-}F_{Drag})$ / D [mN/m]
-3.04934	2.45795	-4.41603	2.49127	-5.08305	1.87687	-17.8478	0.93684	0.00325931	5.31268
-0.867342	1.27644	-2.21345	1.71085	-2.49131	3.48792	-15.6374	1.44186	1.15289	3.13673
0.421874	-0.101634	-0.980607	1.28327	-1.34637	2.71721	-14.3428	1.55056	3.61597	4.68743
2.82726	-0.374782	1.37578	0.955561	1.06035	2.52018	-11.9946	2.37193	6.76621	1.69497
5.34192	-0.406363	3.86014	0.315215	3.45646	2.88969	-9.56552	1.55629	10.002	0.340998
7.68823	-0.393617	6.27087	0.106001	5.81202	3.30913	-7.20433	2.36458	13.1477	0.278913
10.2918	-0.368114	8.60159	0.0303074	8.11226	3.64662	-4.76853	2.89459	16.2634	0.24284
12.5977	-0.352686	11.1357	-0.0312615	10.5322	2.08369	-2.46234	3.16669	19.4021	0.200573
15.2753	-0.319607	13.5513	-0.0719149	13.131	0.112569	0.16319	2.23787	22.6156	0.173566
17.3758	-0.290126	16.031	-0.105811	15.4573	0.0185406	2.42447	3.54197	25.6936	0.144953
20.0615	-0.251849	18.4195	-0.124705	17.828	-0.0404759	4.84199	3.29892	28.9903	0.115833
24.8832	-0.195739	23.1599	-0.150743	22.7457	-0.0741303	9.59095	2.50258	32.5515	0.0974749
30.0388	-0.156071	28.0422	-0.149402	27.49	-0.101546	14.4705	-0.0433041	37.9189	0.0688743
34.9848	-0.12626	32.9543	-0.134158	32.225	-0.101237	20.454	-0.0451092	44.9621	0.0457271
39.6848	-0.109955	37.7567	-0.11584	37.039	-0.0931813	24.0994	-0.064154	50.4092	0.0301445
44.4834	-0.0974393	42.7036	-0.101262	41.676	-0.1085	28.7598	-0.0553626	57.0478	0.0181836
50.7138	-0.0895508	48.661	-0.0886418	47.8065	-0.0896876	34.8473	-0.0489759	66.4075	0.00454936
60.5024	-0.0768863	58.4398	-0.0770632	57.3408	-0.0798143	44.5378	-0.055238	75.4169	-0.0014081
70.3587	-0.0626945	67.9705	-0.07188	66.9934	-0.0792636	54.0885	-0.0342779	85.609	-0.0060518
80.1608	-0.056711	77.9119	-0.067253	76.6519	-0.0609797	63.7206	-0.034812	93.8339	-0.0079515
89.9746	-0.0499927	87.251	-0.0572922	86.4003	-0.0546926	73.3883	-0.0239365	104.119	-0.0054992
99.8004	-0.0428096	97.0766	-0.0561484	95.5675	-0.0485762	83.0477	-0.0208675	113.201	-0.0113215
109.66	-0.0335184	106.905	-0.0484293	105.371	-0.0539168	92.4414	-0.0338661	121.672	-0.0100783
119.327	-0.0393368	116.398	-0.0473238	114.86	-0.0488992	102.203	-0.0248892	132.4	-0.0096173
129.223	-0.0330158	126.424	-0.0468653	124.38	-0.0519593	111.91	-0.023367	141.186	-0.0068021
139.033	-0.029512	135.856	-0.0392867	134.099	-0.0442735	121.304	-0.0217184	150.62	-0.0136936

148.788	-0.0253064	145.831	-0.0310344	143.712	-0.0488042	131.052	-0.00523497	160.433	-0.0102986
158.533	-0.0178333	155.479	-0.0285244	153.319	-0.0490551	140.616	-0.00915747	169.332	-0.0085204
168.361	-0.0273223	164.923	-0.0290664	162.927	-0.0416628	150.353	-0.014511	178.567	-0.0084614
178.431	-0.0232929	174.64	-0.0243942	172.345	-0.0440145	159.63	-0.00352007	188.217	-0.010002
188.039	-0.0209796	184.384	-0.0200288	181.966	-0.0395072	169.514	0.00219765	197.556	-0.0108395
198.029	-0.0216497	194.051	-0.0233994	191.623	-0.0342127	179.152	-0.0108539	209.677	-0.0048149
207.781	-0.017869	203.74	-0.0189751	201.206	-0.0307136	188.636	-0.0260241		
217.594	-0.0220112	213.528	-0.01772	210.699	-0.0365648	198.211	-0.00887407		
227.178	-0.0179603	223.284	-0.0207089	220.349	-0.0283385	207.873	-0.00496459		
237.226	-0.0159989	232.883	-0.0196844	230.135	-0.0296964	217.418	-0.00625421		
246.888	-0.0117561	242.548	-0.016613	239.55	-0.0287593	227.031	-0.0222772		
256.777	-0.0136275	252.262	-0.0156486	249.115	-0.0327955	236.664	-0.0175715		
266.612	-0.0182383	261.936	-0.0135181	258.642	-0.0366608	246.317	-0.0137198		
276.445	-0.0092263	271.617	-0.0165797	268.371	-0.0323875	255.965	-0.0269889		
286.173	-0.0099412	281.281	-0.0153017	277.97	-0.0365044	265.628	-0.0405866		
295.806	-0.0118427	290.962	-0.0114428	287.678	-0.0256401	275.138	-0.0170365		
305.977	-0.0098808	300.678	-0.009602	297.108	-0.037753	284.888	-0.0183513		
315.494	-0.0108845	310.34	-0.0106058	306.674	-0.0299143	294.423	-0.0158603		
325.418	-0.0116122	320.11	-0.0112701	316.365	-0.0223693	304.11	-0.0132373		
335.4	-0.010064	329.886	-0.0077765	325.735	-0.0327252	313.63	-0.0183581		
345.129	-0.0099593	339.538	-0.0038636	335.374	-0.0223946	323.216	0.000621937		
354.757	-0.0135979	349.209	-0.0095301	345.155	-0.0313699	332.769	-0.0179296		
364.544	-0.0107794	358.779	-0.0112492	354.526	-0.0297438	342.326	-0.014395		
374.534	-0.008796	368.712	-0.0056052	364.313	-0.0278782	352.039	0.0035715		
384.165	-0.0089456	378.297	-0.0069544	373.72	-0.0166477	361.649	-0.0259002		
394.09	-0.0058677	387.72	-0.0102114	383.277	-0.016038	371.294	-0.0297561		
403.949	-0.0065312	397.537	-0.009024	392.936	-0.0210404	380.864	-0.0329843		
413.762	-0.0073698	407.16	-0.0099436	402.595	-0.0157806	390.571	-0.035206		
423.475	-0.0074816	416.917	-0.005273	412.226	-0.0230571	400.09	-0.0169907		
433.396	-0.0059927	426.522	-0.004014	421.765	-0.0131681	409.738	-0.043624		
442.991	-0.0073586	436.278	-0.0073827	431.405	-0.0077861	419.279	-0.0272176		
452.966	-0.006405	446.066	-0.0074059	440.867	-0.0139384	428.984	0.00890182		

462.873	-0.0061548	455.834	-0.0055894	450.446	-0.0021338	438.651	-0.0190611
472.499	-0.0087042	465.282	-0.005976	460.026	-0.0130056	448.344	-0.0288901
482.305	-0.0027082	475.181	-0.0042027	469.658	-0.0107415	457.704	-0.000202642
492.233	-0.0047259	484.746	-0.0036626	479.15	-0.0081506	467.389	-0.0381491
501.911	-0.0046231	494.615	-0.0049287	488.891	-0.0110573	476.985	-0.0368085
		504.256	-0.003799	498.474	-0.0072608	486.756	-0.00617622
				508.09	-0.0082156	496.15	-0.0460144
						505.857	-0.0449631

References

(1) Piech, M.; Walz, J. Y. Direct Measurement of Depletion and Structural Forces in Polydisperse, Charged Systems. *J. Colloid Interface Sci.* **2002**, *253*, 117–129, DOI: 10.1006/jcis.2002.8503.

(2) Drelich, J.; Long, J.; Xu, Z.; Masliyah, J.; Nalaskowski, J.; Beauchamp, R.; Liu, Y. AFM Colloidal Forces Measured between Microscopic Probes and Flat Substrates in Nanoparticle Suspensions. *J. Colloid Interface Sci.* **2006**, *301*, 511–522, DOI: 10.1016/j.jcis.2006.05.044.

(3) Tulpar, A.; Van Tassel, P. R.; Walz, J. Y. Structuring of Macroions Confined between Like-Charged Surfaces. *Langmuir* **2006**, *22*, 2876–2883, DOI: 10.1021/la0530485.

(4) Klapp, S. H. L.; Grandner, S.; Zeng, Y.; von Klitzing, R. Charged Silica Suspensions as Model Materials for Liquids in Confined Geometries. *Soft Matter* **2010**, *6*, 2330, DOI: 10.1039/c000194p.